Monte Carlo simulations of diblock copolymer thin films confined between two homogeneous surfaces

Qiang Wang, Qiliang Yan, Paul F. Nealey, and Juan J. de Pablo
Department of Chemical Engineering, University of Wisconsin-Madison, Madison, Wisconsin 53706-1691

(Received 27 July 1999; accepted 30 September 1999)

Thin films of symmetric diblock copolymers confined between two hard, flat and homogeneous surfaces have been investigated by means of Monte Carlo simulations on a simple cubic lattice. For such simulations, the match between bulk lamellar period L_0 and the simulation box size is crucial to obtain meaningful results. The simulations have been performed in an expanded grand-canonical ensemble, where the chemical potential and the temperature of the confined films are specified and the density is allowed to fluctuate. The dependence of morphology, density, and chain conformation in the confined films on the type of surfaces, surface separation, and the strength of surface-block interactions has been studied systematically. Our results are consistent with experimental findings. © *2000 American Institute of Physics.* [S0021-9606(99)51148-3]

I. INTRODUCTION

Diblock copolymer molecules consist of two chemically distinct polymer chains (blocks) covalently bonded at one end. This makes a phase separation in the traditional sense impossible; instead, diblock copolymers undergo order–disorder transitions (ODT) manifested at a microscopic or mesoscopic level. It is now well understood that diblock copolymer melts exhibit a variety of ordered structures; the resulting microphase-separated states depend on the composition of the polymer. In the case of symmetric diblock copolymers, where A and B blocks have the same volume fraction, the equilibrium ordered structure is a spatially periodic lamellar structure characterized by an alternating arrangement of A-rich and B-rich layers, i.e., $A-B$, $B-A$, $A-B$, etc.

Recently, the study of diblock copolymer thin films has attracted significant interest because of their potential applications in nano-fabrication. Most research has been carried out on symmetric diblock copolymers. In the bulk, such copolymers exhibit a characteristic period of lamellar microdomains (denoted by L_0) at temperatures below the ODT. In the case of diblock copolymer thin films, the tendency to form lamellae with the bulk period, surface-block interactions, and confinement by surfaces, all have important effects on the morphology of the films, thereby making them radically different from their bulk counterparts.

In general, the interactions between the surfaces and the two blocks are different; the surfaces preferentially attract one of the two blocks, and lamellae orient parallel to the surfaces. The number of bilayers of parallel lamellae is an integer if the same blocks are preferred by both surfaces (similar surfaces), or half an odd integer if different blocks are preferred by the two surfaces (dissimilar surfaces). When the top surface is free (e.g., air), the frustration between film thickness (denoted by D) and L_0, i.e., the fact that D/L_0 is not an integer for similar surfaces or half an odd integer for dissimilar surfaces, can be released by forming islands and holes on the free surface. However, the formation of islands and holes is suppressed by confining the copolymers between two hard (impenetrable) surfaces. In this case, the frustration between surface separation D and bulk lamellar period L_0 may force the copolymers to change the period of the confined lamellae (denoted by L) from L_0, or to adopt a different lamellar orientation.

Experimental studies of diblock copolymer thin films confined between two hard and homogeneous surfaces show that, due to the strong tendency by the surface to preferentially attract one of the two blocks, the lamellae tend to orient parallel to the surfaces.[1–3] When the same blocks are preferred by both surfaces, the number of bilayers within the parallel lamellae (denoted by n) is an integer between $D/L_0-\frac{1}{2}$ and $D/L_0+\frac{1}{2}$. When D/L_0 is not an integer, the confined lamellar period L deviates from L_0 to accommodate the frustration. The confined lamellae are compressed and stretched in a cyclic manner as a function of D.[1–3] A first-order transition appears to occur between the compressed and the stretched states of the copolymer chains.[1,2] Further experiments also show that, as surface-block interactions become less specific, an additional increase in the frustration between D and L_0 can lead to formation of perpendicular lamellae with $L \approx L_0$ near at least one of the surfaces.[3,4] TEM images show that the perpendicular orientation is short-ranged.[3,4] Huang *et al.* studied experimentally symmetric diblock copolymer thin films confined between two neutral surfaces.[5] Perpendicular lamellae were observed throughout the entire film.[5] These experiments are discussed in more detail in Sec. V.

Several years ago Kikuchi and Binder performed Monte Carlo simulations of symmetric diblock copolymer thin films confined between two identical, hard, homogeneous, and parallel surfaces with weak repulsion to one of the two blocks (symmetric surfaces).[6,7] A simple cubic lattice model was used in their simulations. Due to the surface preference, lamellae were found to align parallel to the surfaces when the frustration between the surface separation and L_0 was small. The number of bilayers of the parallel lamellae, which is an

integer in their simulations, was found to be a function of the surface separation.[6,7] In the case of strong frustration between the surface separation and L_0, these authors found tilted or deformed lamellar structures, and even coexistence of lamellae having different orientations.[6,7] However, our calculations indicate that there was a significant mismatch between L_0 and the simulation box size used in their simulations, which could have influenced the reported perpendicular structures. This issue is addressed in more detail in Sec. III.

Theoretical studies have also been conducted to understand the morphology of symmetric diblock copolymer thin films confined between two hard, homogeneous, infinite and parallel surfaces. For two neutral surfaces having no preference for either one of the two blocks, perpendicular lamellae have been predicted to be the most stable morphology, regardless of the surface separation.[8,9] Pickett and Balazs explained this by the nematic ordering of the segments near the surfaces that arises from the orientational constraint imposed by the hard surfaces.[8] Matsen attributed this behavior to the existence of a negative line tension where the $A-B$ interfaces intersect the surfaces.[9]

For the case of two identical surfaces with preferential surface-block interactions (symmetric surfaces),[8–13] parallel symmetric lamellae (configurations with an integer number of bilayers) and perpendicular lamellae with the bulk period have been predicted theoretically, depending on the extent of frustration between D and L_0 and the strength of the surface preference. If the surface preference is weak, perpendicular lamellae occur when parallel symmetric lamellae are least favorable as the frustration between D and L_0 increases.[8,9,12,13] For the perpendicular structure, preferential segregation of the wetting blocks to both surfaces is predicted, which causes some oscillation of the $A-B$ interfaces.[8,9,13] The parallel antisymmetric lamellae (configurations with half an odd integer number of bilayers) predicted by Turner[11] are never favored, but they are metastable whenever a perpendicular structure is anticipated.[8,9,12,13] Increasing the surface preference leads to a breakdown of the perpendicular structure in favor of the parallel symmetric one for fixed surface separations.[9,12,13]

For the case of two dissimilar surfaces preferring different blocks, there exists a limited regime over which parallel antisymmetric lamellae can be found.[9,12,13] Again, perpendicular lamellae have been predicted when parallel lamellae are least favorable as the frustration increases.[9,12] In their Cahn–Hilliard calculations of antisymmetric surfaces (two surfaces attract opposite blocks with the same strength of surface-block interaction), Brown and Chakrabarti observed perpendicular structures which were in some cases significantly different from well-formed perpendicular lamellae.[13]

Matsen developed a self-consistent-field theory to examine complex morphology in thin films of diblock copolymers.[9] He found that for symmetric diblock copolymers, the mixed lamellar phases encountered in the experiments[4] and Monte Carlo simulations[7] are slightly unstable relative to perpendicular lamellae. But a small asymmetry in the diblock copolymer molecules stabilizes a mixed lamellar phase. This raises the possibility that the mixed lamellar phases observed in the experiments and simulations are kinetically favored, rather than true equilibrium structures.[9] However, we have a slightly different point of view regarding the formation of the mixed morphology. We also address this issue in Sec. V.

Monte Carlo simulations of confined copolymer thin films could provide valuable insights regarding molecular configurations in such systems; that information is difficult to extract from experiment or theory. Simulations could also validate theoretical predictions, which necessarily involve a series of approximations. Unfortunately, to the best of our knowledge, only one simulation study of confined copolymers has appeared in the literature.[6,7] As discussed in Sec. III, it is possible that the simulation box size employed by Kikuchi and Binder might have adversely influenced some of their results. Furthermore, their simulations were performed in a canonical ensemble (NVT simulations), where it is not possible to consider density fluctuations in the confined films.

In this paper, we present results of Monte Carlo simulations of symmetric diblock copolymer thin films confined between two hard, homogeneous and parallel surfaces. Such simulations were performed in an expanded grand-canonical ensemble. The confined copolymers were in equilibrium with a bulk phase having a specified chemical potential and temperature. The density of the confined thin film was thus allowed to fluctuate during the simulation. We focus on the dependence of the morphology, density, and chain conformation in the confined films on the film thickness and the strength of the surface preference. This paper is organized as follows: In Sec. II we describe the model and the simulation methodology. In Sec. III we discuss the match between L_0 and simulation box size, which is crucial for simulations of lamellar structures with periodic boundary conditions (PBC), and the anisotropy of a cubic lattice. In Sec. IV we present the major results of our simulations for confined films. In Sec. V we qualitatively compare our simulations with experimental results, and address the issue of the mixed morphology. The last section provides a summary.

II. MODEL

A. Simple cubic lattice model

We use a simple cubic lattice model in our simulations. A symmetric diblock copolymer chain consists of the same number of A and B segments connected by bonds whose length is taken to be the lattice unit. Each segment occupies one lattice site, and each lattice site is occupied by at most one segment. A rectangular simulation box of dimensions L_x, L_y, and L_z is employed. Periodic boundary conditions (PBC) are imposed in the x and y directions. For simulations in the bulk, PBC are also imposed in the z direction. To simulate a confined film, two flat and homogeneous surfaces are introduced through the lattice sites at $z=0$ and $z=L_z+1$, respectively, as shown in Fig. 1. To represent hard surfaces, these lattice sites are not allowed to be occupied by polymer segments. Diblock copolymers are therefore confined to a thin-film geometry of thickness $D=L_z-1$.

In our model, we only consider repulsion between nearest-neighbor $A-B$ pairs separated by one lattice unit

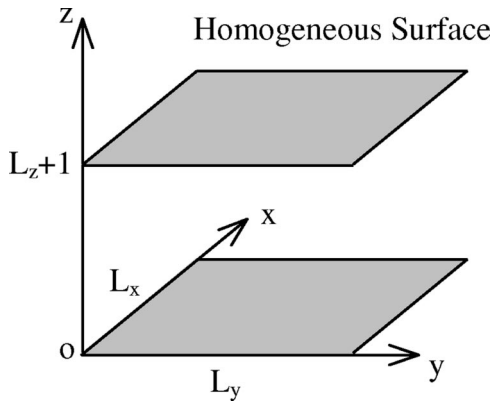

FIG. 1. Surface configuration for confined films. Each surface can be sA (repelling B blocks), sB (repelling A blocks) or neutral surface.

$(\epsilon_{A-B}>0)$, and we set $\epsilon_{A-A}=\epsilon_{B-B}=0$. Interactions between vacancies (unoccupied lattice sites) and polymer segments are also set to zero. Three kinds of sites populate the surfaces: sA, sB, and sN, whose nature depends on the type of surface-block interactions. For simplicity, we set $\epsilon_{sN-A}=\epsilon_{sN-B}=\epsilon_{sA-A}=\epsilon_{sB-B}=0$, and $\epsilon_{sA-B}=\epsilon_{sB-A}=\alpha\epsilon_{A-B}$, where $\alpha>0$. The larger the value of α, the stronger the surface-block repulsion. A homogeneous surface consisting of sN sites is neutral, with no preference for either of the two blocks. A homogeneous surface consisting of sA sites (referred to as the ''sA surface'') repels B segments, and is therefore preferential to A segments, and vice versa. The difference between ϵ_{sA-A} and ϵ_{sA-B} (ϵ_{sB-A} and ϵ_{sB-B}) can be viewed as a chemical potential difference between the two species at the sA (sB) surface. The total energy in our system is given by

$$E=n_{A-B}\epsilon_{A-B}+n_{sA-B}\epsilon_{sA-B}+n_{sB-A}\epsilon_{sB-A},$$

where n_{A-B} is the number of nearest-neighbor $A-B$ pairs, n_{sA-B} is the number of nearest-neighbor B segments to the sA surface, and n_{sB-A} is the number of nearest-neighbor A segments to the sB surface.

B. Simulations in an expanded grand-canonical ensemble

We perform Monte Carlo simulations in a variant of the expanded grand-canonical ensemble method proposed by Escobedo and de Pablo.[14] The chemical potential and temperature of the simulated system are specified prior to a simulation. The confined copolymers are therefore in equilibrium with a bulk phase having the same chemical potential and temperature, and the density of the system is allowed to fluctuate during the simulation. In addition to molecule displacements by reptation moves and local (crankshaft and kink-jump) moves, we employ growing/shrinking moves in our simulations to gradually insert/remove particles from the system.

During a simulation, the system consists of N_c-1 normal chains of length N and a tagged chain. The length of the tagged chain is allowed to fluctuate between 0 and N. Instead of creating or annihilating a whole chain in a single step, growing or shrinking moves are attempted for the tagged chain. In each of these attempts, two pieces consisting of m A and m B segments, respectively, are appended to or removed from the corresponding ends of the tagged chain. If the tagged chain grows into a full chain of length N, it turns into a normal chain; a new zero-length tagged chain is then created. On the other hand, if the tagged chain shrinks to zero length, a randomly chosen normal chain becomes tagged. To facilitate transitions, configurational bias is used for these growing/shrinking moves, as described below.

A tagged molecule can have M different states. States $y=1$ and $y=M$ correspond to a zero-length and a full-length chain, respectively. Other states are related to the instantaneous length of the tagged chain $r(y)$ by $r(y)=2m(y-1)$. Growing/shrinking trial moves are accepted with probability:

$$P_{\text{accept}}=\min[1,(W_R)^{\delta}\exp(\Psi_{y+\delta}-\Psi_y)\exp(-\beta\Delta U)], \tag{1}$$

where W_R is the Rosenbluth weight associated with the growth process if $\delta=+1$ and with the hypothetical reverse growth process if $\delta=-1$. The Rosenbluth weight is given by

$$W_R=\prod_{i=r_A+1}^{r_B}\frac{n(i)}{z},$$

where $r_A=\min[r(y),r(y+\delta)]$, $r_B=\max[r(y),r(y+\delta)]$, $n(i)$ is the number of unoccupied sites for the ith segment around the previous $(i-1)$th segment of the tagged chain, and $z=6$ for a simple cubic lattice. In Eq. (1), Ψ_y is the preweighting factor for state y, given by

$$\Psi_y=\frac{y-1}{M-1}\left(\beta\mu-\ln\frac{N_c}{V}\right), \tag{2}$$

where N_c is the total number of chains in the system, including the tagged chain if $y\neq 1$; $\beta\equiv 1/(k_BT)$, k_B is Boltzmann's constant, and T is the absolute temperature; μ is the specified chemical potential and V is the volume. In Eq. (1), ΔU is the energy change caused by a growing/shrinking trial move.

The ''chunk size'' m is an important parameter in expanded grand-canonical ensemble simulations. A small value of m can lead to an unnecessarily large number of intermediate states, while a large value can cause a low acceptance ratio. If $m=N/2$, the expanded grand-canonical ensemble reduces to a conventional grand-canonical ensemble. We optimized the chunk size in a manner similar to that outlined in Ref. 15, and found an optimal value of $m=2$ for our system, which leads to an acceptance ratio of about 20% for the growing/shrinking moves in our simulations.

For dense polymer melts, growing/shrinking moves accelerate the equilibration of the system. According to our calculations, the number of Monte Carlo steps (defined below) needed for equilibration in the expanded grand-canonical ensemble is about half of that required in NVT simulations. Growing/shrinking moves also help prevent the system from getting trapped in configurations corresponding to local energy minima. In our simulations we observed multiple transitions from one type of morphology to another even after the system had reached a locally stable state. More importantly, simulations in the expanded grand-canonical ensemble allow us to study density changes of the confined films. This is not possible in NVT simulations.

We study symmetric diblock copolymers of chain length $N=24$. We set the reduced chemical potential at $\mu^* \equiv \beta\mu = 41.5$ for all the simulations in the expanded grand-canonical ensemble. In the range of temperatures studied here, this leads to densities of thin films (percentage of occupied lattice sites in our system) of around 0.8, which correspond to highly concentrated copolymer solutions or melts.[16] A standard Metropolis algorithm is employed in our simulations. One Monte Carlo step (MCS) consists of $0.8 \times L_x \times L_y \times L_z$ trials of reptation, local and growing/shrinking moves, each of which occurs with the same probability. In general, we discard the first 100 000 MCS for equilibration, then make a run of 500 000 MCS while collecting data every 5 MCS.

C. Characterization of morphology

1. Order parameter profile

To characterize the morphology observed in our simulations, we calculate the order parameter profiles along the x, y, and z directions. The order parameter profile along the x direction, for example, is $\langle \rho_A(x) - \rho_B(x) \rangle$, where $\rho_A(x)$ is the percentage of lattice sites occupied by A segments in the cross section of a $y-z$ plane at a given x, and $\langle\ \rangle$ represents an average over all the collected configurations (after equilibration).

For lamellar structures, we can use the normal to the $A-B$ interfacial plane (referred to as the ''normal of the lamellae'') to represent the orientation of the lamellae. The order parameter profile along the direction of this normal features the spatially alternative arrangement of A-rich and B-rich layers. Since the density of our films is around 0.8, the maximum and minimum value of the order parameter profile along this direction should be close to 0.8 (in A-rich layers) and -0.8 (in B-rich layers), respectively, and the period of the oscillation of the order parameter profile is equal to the lamellar period, provided that a lamellar structure is well developed (along this direction) in our simulation.

When there is a translational symmetry along the direction of the normal of the lamellae, the $A-B$ interfaces have no preferred location (in the fixed coordinates) along that direction. Therefore, in order to keep the oscillating feature of the order parameter profiles along this direction from being smeared out by the average (in the fixed coordinates), we aligned the order parameter profile of each configuration by starting from the cross section where the maximum value of the order parameter profile occurs. For example, in the case of perpendicular lamellae forming along the x direction, in which PBC are imposed, $\rho_A(x^*) - \rho_B(x^*)$ always has its maximum value at $x^*=1$ for each collected configuration, where x^* is the aligned coordinate. Such an aligned order parameter profile, denoted by $\langle \rho_A(x^*) - \rho_B(x^*) \rangle$, captures lamellar features unequivocally. Due to morphology irregularities, such aligned order parameter profiles have a small positive value in the region near $x^*=1$ even if there is no lamellar structure along the x direction at all. This, however, does not affect our analysis qualitatively. In this paper, the order parameter profiles in the x and y directions are always aligned. Those in the z direction are also aligned for simulations in the bulk, but not aligned for simulations in the confined films.

2. Orientation profile of diblock copolymer chains

We define an orientation vector pointing from the center-of-mass of A block to the center-of-mass of B block (on the same molecule) to describe the orientation of a diblock copolymer chain. Since we are only concerned with the orientation of chains relative to the surfaces, we calculate $\langle |\cos\theta(z)| \rangle_b$ and $\langle \cos\theta(z) \rangle_b$, where $0 \leqslant \theta(z) \leqslant \pi$ is the angle between the direction of the z axis and the orientation vector of a chain whose center-of-mass (for the whole chain) is located between $z-0.5$ and $z+0.5$ ($z=1,2,\ldots,L_z$) in any given configuration of the system; $\langle\ \rangle_b$ is an average over all such chains in each collected configuration, and over 1000 successively collected configurations (which correspond to 5000 MCS for simulations in the expanded grand-canonical ensemble). Such an average can provide us with qualitative and ''instantaneous'' information of some locally stable morphology.

In perpendicular lamellae (along either the x or y direction), chains are mainly parallel to the surfaces, and therefore $\theta(z) \approx \pi/2$, $\langle |\cos\theta(z)| \rangle_b \approx 0$, and $\langle \cos\theta(z) \rangle_b \approx 0$. In parallel lamellae, chains are mainly perpendicular to the surfaces, and therefore $\theta(z) \approx 0$ or π, $\langle |\cos\theta(z)| \rangle_b \approx 1$, and $\langle \cos\theta(z) \rangle_b \approx 1$ [in the case of $\theta(z) \approx 0$] or -1 [in the case of $\theta(z) \approx \pi$]. Due to morphology irregularities, we choose $\langle |\cos\theta(z)| \rangle_b = (1/\pi) \int_0^\pi |\cos\theta| d\theta = 2/\pi$ as the criterion between the perpendicular and parallel orientations of the chains. This quantity is represented by a dotted line in the subsequent figures of chain orientation profiles.

3. Center-of-mass distribution of chains along the z direction

We also calculate the chain center-of-mass distribution along the z direction, denoted by $\langle D(z) \rangle_b$. For a collected configuration of the system, $D(z) = N_c(z)/N_c$, where $N_c(z)$ is the number of chains whose center-of-mass (for the whole chain) lies between $z-0.5$ and $z+0.5$ ($z=1,2,\ldots,L_z$). [Different from Eq. (2), here N_c does not include the tagged chain.] For parallel lamellae, the center-of-mass distribution fluctuates along the z direction; most chains have their center-of-mass in the middle of each layer of copolymer molecules, and only a few chains have their center-of-mass between two neighboring layers of molecules.

III. EFFECTS OF PBC AND ANISOTROPY OF CUBIC LATTICE

It has been pointed out[17,18] that for lattice simulations of lamellar structures with periodic boundary conditions (PBC), the match between the periodicity of the lamellae and the PBC is crucial to obtain meaningful results. The spatially periodic structure of lamellae induces long-range interactions between A and B blocks. In simulations of such systems, the meaning of imposing PBC when the periodicity of lamellae and PBC are not properly matched is unclear. If they are mismatched, PBC could change the characteristic (''true'')

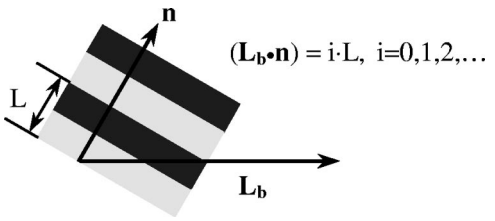

FIG. 2. Match between PBC and lamellar period L.

period of the lamellae, or even the morphology of the diblock copolymers, until these become consistent with PBC. In that event, the simulated morphology would be an artifact of the PBC, and not the ''true'' morphology that would correspond to a system of infinite size. The observed ''buckling'' of lamellae[17] is a manifestation of this problem.

The periodicity of PBC can be represented by a vector $\mathbf{L_b} \equiv L_b \mathbf{n_i}$, where $\mathbf{n_i}$ is the direction in which PBC are imposed, and L_b the length of the simulation box in that direction. As shown in Fig. 2, the match between periodicity of lamellae and PBC requires that the projection of $\mathbf{L_b}$ in the direction of the normal of the lamellae $\mathbf{n}$, $(\mathbf{L_b} \cdot \mathbf{n})$, be an integer multiple of the lamellar period L. This should be satisfied for all the directions in which PBC are imposed.

In the first published simulations of confined symmetric diblock copolymers, Kikuchi and Binder performed Monte Carlo simulations in a simple cubic lattice (the same as employed in this work) of thin films between two identical, hard, homogeneous (preferential) and parallel surfaces.[6,7] Their simulation box size was $L_x \times L_y \times D$, where $L_x = L_y$ are the lengths in the x and y directions, respectively, in which PBC are imposed, and where D is the length in the z direction. They observed tilted or deformed lamellar structures, and even coexistence of lamellae in different orientations in the case of strong frustration between surface separation and L_0.[6,7] However, since in their simulations L_x and L_y were chosen to be 24, while the characteristic period of the lamellae was estimated to be $L_0 \approx 10$ (at the temperature of $1/T^* \equiv \epsilon_{A-B}/k_BT = 0.6$),[6,7] the issue of mismatch between PBC and L_0 could have influenced the reported perpendicular structures. While these authors did conduct simulations with another box size, namely $L_x = L_y = 16$, to explore finite-size effects in their results,[6,7] the problem of mismatch could persist for that particular box size.

Prior knowledge of L_0 is crucial to prevent such a mismatch in simulations with periodic boundary conditions (PBC). However, estimating L_0 accurately from bulk simulations is difficult, as we shall see below. This problem can be partially alleviated by using large systems, but this requires longer and more demanding calculations.

To estimate L_0 for our symmetric diblock copolymers of chain length $N = 24$, we performed bulk simulations in the expanded grand-canonical ensemble with four different simulation boxes ($25 \times 27 \times 24$, $26 \times 28 \times 24$, $26 \times 30 \times 24$, $27 \times 28 \times 24$) at three reduced temperatures, namely $T^* \equiv k_BT/\epsilon_{A-B} = 2.2$, 2.3, and 2.4. In a different series of simulations we had found the ODT of the copolymers to be in the range $T^* = 2.8 \sim 3.0$. These temperatures are therefore in the intermediate segregation regime. We conducted five runs for each simulation box at each temperature, with the only difference being the random number generator seed. The chemical potential of the copolymers was set to be $\mu^* = 41.5$ for all these simulations. The observed lamellar configurations for these boxes are shown in Table I. The observed density versus lamellar period for these bulk simulations is shown by the open symbols in Fig. 3.

In these bulk simulations, we observed different lamellar periods in different simulation boxes. Even for identical

TABLE I. Observed (simulated) lamellar configurations in different simulation boxes. Each row represents a different bulk lamellar configuration corresponding to the box size given in the left column. (Some distinct runs gave the same configuration. See text for simulations conducted in each box.) n_x, n_y, and n_z represent the number of lamellar periods contained in the simulation box along each axis. For a given observed set of n_x, n_y, and n_z, the observed L_0, which is rounded to three decimals in the table, is determined from $1/\sqrt{(n_x/L_x)^2+(n_y/L_y)^2+(n_z/L_z)^2}$, where L_x, L_y, and L_z are the simulation box dimensions. The rows in gray background highlight lamellar configurations where the A–B interfacial plane is parallel to two of the three axes of the corresponding simulation box. The rows in shaded background and bold fonts highlight lamellar configurations where the A–B interfacial plane is parallel to none of the three axes of the corresponding simulation box. Some other possible lamellar configurations have not been observed in our bulk simulations.

Box Size	Observed L_0	n_x	n_y	n_z
25×27×24	12.5	2	0	0
	12	0	0	2
	11.879	1	2	0
	11.766	0	2	1
26×28×24	13	2	0	0
	12.327	1	2	0
	12.093	0	2	1
	12	0	0	2
	11.791	2	1	0
	11.431	2	0	1
26×30×24	13	2	0	0
	12.993	1	2	0
	12.720	0	2	1
	12	0	0	2
	11.928	2	1	0
	11.431	2	0	1
	11.426	**1**	**2**	**1**
	11.142	0	1	2
27×28×24	12.429	1	2	0
	12.160	2	1	0
	12.093	0	2	1
	12	0	0	2
	11.766	2	0	1
50×51×48	12.355	1	4	0
	12.323	0	4	1
	12.141	4	1	0
	12.130	**2**	**3**	**2**
	12	0	0	4
	11.965	**1**	**4**	**1**
	11.915	**2**	**2**	**3**

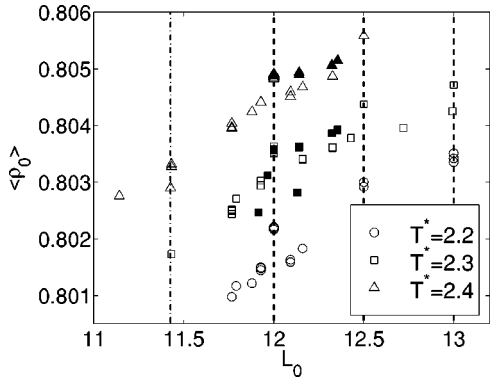

FIG. 3. Results of bulk simulations in five simulation boxes listed in Table I. Open symbols denote results in the four small simulation boxes; filled symbols denote results in the large simulation box. Symbols in the same shape represent results under the same temperature. See text for more explanation.

simulation boxes, we sometimes found different lamellar periods in different runs. From the $\langle\rho_0\rangle$-L_0 data shown in Fig. 3 we cannot tell which value of the observed L_0 is nearest to the ''true'' L_0. From Fig. 3 we can see that $\langle\rho_0\rangle$ increases as the observed L_0 increases. However, there seem to be some peaks at $L_0=12$, 12.5, and 13 (shown by the dashed lines in Fig. 3); $\langle\rho_0\rangle$ is notably high at these values of L_0. To explain this result, we use the $A-B$ interfacial plane to represent the orientation of the lamellae. For all the observed L_0's represented by the open symbols in Fig. 3 except those on the dashed and dashed–dotted lines, the $A-B$ interfacial plane in the corresponding lamellar configuration is parallel to only one of the three axes, in which direction the number of lamellar periods is 0 (as shown in Table I). For $L_0=12$, 12.5, and 13, the $A-B$ interfacial plane is parallel to two of the three axes, that is, it is parallel to either the $x-y$, $y-z$, or $x-z$ plane of our simulation boxes. These configurations lead to notably high values of $\langle\rho_0\rangle$. In addition, for $L_0\approx11.426$ (shown by the dashed–dotted line in Fig. 3, only one data point for $T^*=2.4$), the $A-B$ interfacial plane actually intersects all three axes, that is, it is not parallel to any of them. This configuration leads to a notably low value of $\langle\rho_0\rangle$. It seems that the difference within each ''class'' of lamellar configurations is relatively negligible for these small boxes.

Similar results were observed when we used a larger simulation box of $50\times51\times48$. We conducted nine and five runs in this simulation box at $T^*=2.3$ and 2.4, respectively, with the only difference being the random number generator seed. The chemical potential of the copolymers was also set to be $\mu^*=41.5$ for all these simulations. The observed lamellar configurations in this box are also shown in Table I. The observed density versus lamellar period for these bulk simulations is shown by the filled symbols in Fig. 3. Similarly, for $L_0=12$ (one data point for each temperature), the $A-B$ interfacial plane is parallel to the $x-y$ plane of our simulation box. This configuration leads to a notably high value of $\langle\rho_0\rangle$. For $L_0\approx11.915$, 11.965, and 12.130 (three data points observed only at $T^*=2.3$), the $A-B$ interfacial plane actually intersects all three axes. These configurations lead to notably low values of $\langle\rho_0\rangle$. Note that the result corresponding to $L_0\approx11.965$ is even notably different from the other two. In addition, we can see that, as expected, the range of the observed L_0 in the large simulation box is much smaller than that in the small ones.

The above observations suggest that the observed peaks in $\langle\rho_0\rangle$ reflect the anisotropy of the simple cubic lattice model. The bonds connecting copolymer segments can only be oriented along one of the three axes of the simple cubic lattice; different orientations of lamellae in the lattice may therefore lead to different results. To minimize the effects of such anisotropy, we choose to work with simulation boxes where only the lamellae parallel to two axes can be developed in our simulations.

From Fig. 3 we can also see that, at the same bulk density, the observed L_0 decreases as T^* increases. This is consistent with the relationship between ''true'' L_0 and T^*: the characteristic period of lamellae decreases as temperature increases. From our bulk simulation results shown in Fig. 3 we can see that the observed L_0's are all distributed around 12; the scatter of our results around 12 is even smaller for the large simulation box, where the effects of anisotropy of the lattice model are less pronounced. In light of these observations, throughout the remainder of this work we simply assume that $L_0=12$ (at $T^*=2.3$ and $\mu^*=41.5$; these thermodynamic conditions are fixed throughout all subsequent simulations of confined films). This value is well within the range of all of our bulk simulation results. Furthermore, we choose $L_x=L_y=24$, i.e., an integer multiple of L_0. As we shall see below, only perpendicular and parallel orientations of lamellae are observed in such simulation boxes.

It is important to point out, however, that even after a judicious choice of box dimensions, finite-size effects are reduced but not completely absent in our simulations. In order to eliminate them completely, simulations in much larger boxes would be necessary; unfortunately, calculations of that magnitude are beyond the reach of available computational resources.

IV. RESULTS AND DISCUSSION

In this section, we present the major results of simulations of symmetric diblock copolymer thin films confined between two hard, homogeneous, and parallel surfaces. Three kinds of surface configurations are considered here: neutral surfaces (both surfaces consist of sN sites), symmetric surfaces (two identical surfaces consist of sB sites repelling A segments), and antisymmetric surfaces (the lower surface consists of sB sites repelling A segments, and the upper surface consists of sA sites repelling B segments; both surfaces repel the corresponding segments with the same strength of surface-block interactions). The surface separation varies from L_0 to $3L_0$ in steps of $0.25L_0$. In the case of symmetric and antisymmetric surfaces, two values of α $(=\epsilon_{sA-B}/\epsilon_{A-B}=\epsilon_{sB-A}/\epsilon_{A-B})$, 0.5 and 2, are used to represent a weak and a strong surface preference, respectively. The morphology of the confined diblock copolymer thin films, the density of the films, the mean square end-to-end distance of the copolymer chains, and the surface-induced preferential segregation of the segments are discussed in each of the following sections.

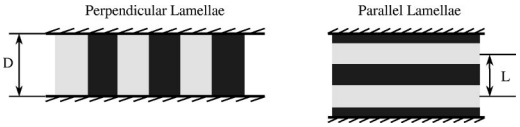

FIG. 4. Two types of stable morphology observed between two neutral, symmetric, and antisymmetric surfaces.

A. Morphology of confined symmetric diblock copolymer thin films

As illustrated in Fig. 4, two types of stable morphology are found in our simulations: perpendicular lamellae and parallel lamellae. For perpendicular lamellae, the confined lamellar period L is always equal to the bulk value L_0. For parallel lamellae, $L=D/n$, where D is the film thickness, and n the number of bilayers of parallel lamellae within the confined films. (We assume here that all the half-layers in the parallel lamellae have the same thickness.) We found in our simulations that n is always an integer in the case of symmetric surfaces, and half an odd integer in the case of antisymmetric surfaces. Therefore, for parallel lamellae, L can deviate from L_0 if frustration occurs between D and L_0. It is useful to define a parameter f to measure the extent of such frustration; assuming that parallel lamellae of n bilayers form throughout the thin film, we define $f \equiv D/(nL_0)-1 = (L-L_0)/L_0$. We can see that $f>0$ when the parallel lamellae are stretched, and $f<0$ when the parallel lamellae are compressed. Furthermore, the larger the absolute value of f, the stronger the frustration. Note that f is a function of D/L_0 only. As we shall see later, the value of n is adopted by the system in such a way as to minimize the extent of frustration. Even when perpendicular lamellae actually form, f can still be calculated as indicated above.

In our simulations for two neutral surfaces with no preference for either of the two blocks, perpendicular lamellae with $L=L_0$ are found throughout the entire film for all surface separations, even at $f=0$. This is consistent with predictions from self-consistent-field calculations.[8,9] Shown in Fig. 5(a) are the chain orientation and center-of-mass distribution profiles in the perpendicular lamellae between two neutral surfaces separated at $D/L_0=2$. We obtain similar results for all other surface separations studied here. Since copolymer molecules cannot penetrate the hard surfaces, chains close to the surfaces prefer to assume a parallel orientation. This can be seen from the profile of $\langle|\cos\theta(z)|\rangle_b$. In the interior of the confined film (from $z=3$ to L_z-2), $\langle|\cos\theta(z)|\rangle_b$ has a small positive value of about 0.38 caused by the fluctuation of $\theta(z)$. In the immediate vicinity of the surfaces (at $z=1$ and L_z), however, it is almost 0. Because of the entropy loss of chains near the surfaces, few chains have their center-of-mass very close to the surfaces. Therefore, $\langle D(z)\rangle_b$ is also almost 0 there, but exhibits a peak slightly away from the surfaces (at $z=2$ and L_z-1). We refer to this phenomenon as the ''hard-surface effect.'' Such an effect induces the formation of perpendicular lamellae near neutral surfaces.

The hard-surface effect is also observed in the case of parallel lamellae between two hard (preferential) surfaces. Shown in Fig. 5(b) are the chain orientation and center-of-mass distribution profiles in the parallel lamellae between symmetric and strongly preferential surfaces separated at $D/L_0=2$. We can also see that $\langle|\cos\theta(z)|\rangle_b$ and $\langle D(z)\rangle_b$ are almost 0 at $z=1$ and L_z, due to the hard-surface effect. In this case, however, this effect is somewhat suppressed by the formation of parallel lamellae. We can see that the slope of $\langle|\cos\theta(z)|\rangle_b$ at $z=1$ and L_z in Fig. 5(b) is larger than that in Fig. 5(a). Also, there is no peak of $\langle D(z)\rangle_b$ at $z=2$ and L_z-1 in Fig. 5(b).

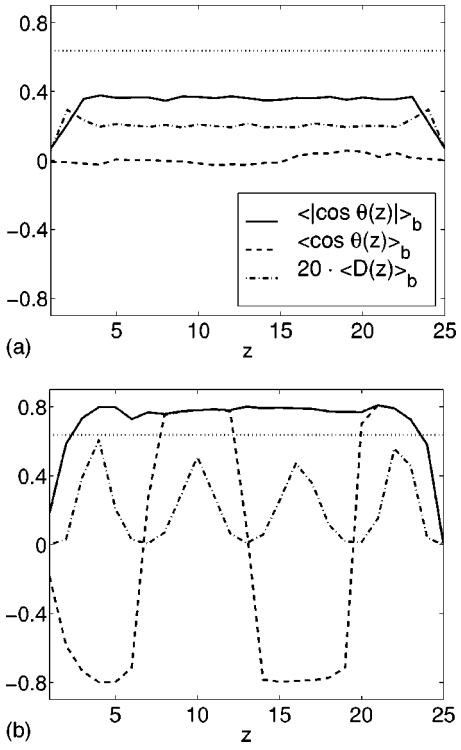

FIG. 5. Chain orientation and center-of-mass distribution profiles in (a) perpendicular lamellae between two neutral surfaces at $D/L_0=2$; (b) parallel lamellae between symmetric and strongly preferential surfaces at $D/L_0=2$. The legend is the same as in (a). In both figures, the dotted line represents the criterion between the perpendicular and parallel orientations of chains: $\langle|\cos\theta(z)|\rangle_b=(1/\pi)\int_0^\pi|\cos\theta|d\theta=2/\pi$.

Figure 6 summarizes the morphology of confined films between two hard and homogeneous (preferential) surfaces. We can see that the confined morphology depends on the nature of surface-block interactions and the extent of frustration between D and L_0. As the surface preference increases, lamellae exhibit a stronger tendency to be parallel to the surfaces; the preferred blocks segregate near the corresponding surfaces to decrease the surface-block interfacial energy. Consequently, n is always an integer (parallel symmetric lamellae) in the case of symmetric surfaces or half an odd integer (parallel antisymmetric lamellae) in the case of antisymmetric surfaces, as shown in Fig. 6. This is consistent with results found in the literature.[2,9,12,13] Parallel antisymmetric lamellae between symmetric surfaces and parallel symmetric lamellae between antisymmetric surfaces are never found in our simulations; in such morphology the surface-block interfacial energy at one of the surfaces would be too high. In parallel lamellae, any frustration between D and L_0 is accommodated by deviations of L from L_0. Com-

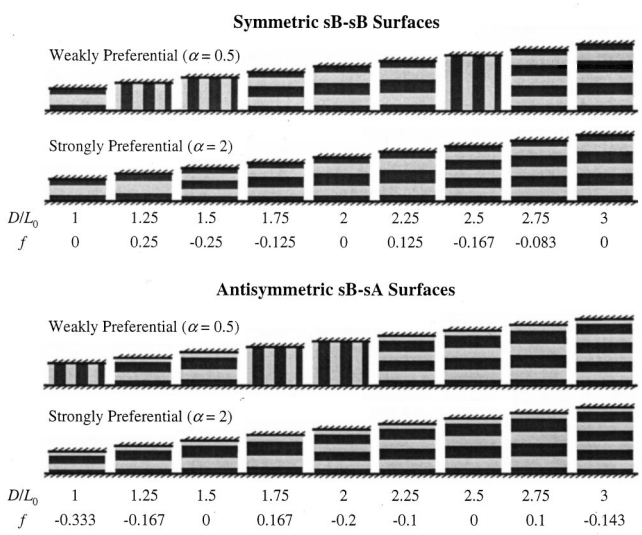

FIG. 6. Illustration of the morphology of symmetric diblock copolymer thin films confined between two hard and homogeneous (preferential) surfaces. Light regions represent A blocks and dark regions represent B blocks. f measures the frustration between surface separation D and bulk lamellar period L_0. Refer to the text for its definition. For two neutral surfaces with no preference for either of the two blocks, perpendicular lamellae with $L = L_0$ are found throughout the entire film for all surface separations.

pressing or stretching the confined parallel lamellae would cost some elastic energy (conformational entropy). This cost is minimized by choosing an appropriate value of n. This is why confined parallel lamellae are compressed and stretched in a cyclic manner as a function of D.

From the results shown in Fig. 6 for two weakly preferential surfaces, we can see that there exists a maximum absolute value of f for the formation of parallel lamellae, denoted by $|f|^{=}_{\max}$. This value corresponds to the maximum extent to which lamellae may be compressed or stretched by the surfaces. For those surface separations for which $|f|$ is larger than $|f|^{=}_{\max}$, the diblock copolymers would not accommodate such frustration by excessively compressing or stretching the lamellae parallel to the surfaces. Instead, they change their orientation to form perpendicular lamellae of $L = L_0$, at the lesser cost of increasing the surface-block interfacial energy. This change of orientation is a manifestation of the competition between tendencies to form lamellae with the bulk period and to decrease the surface-block interfacial energy.[8,9,12,13]

Our results also indicate that $|f|^{=}_{\max}$ increases as the surface preference increases. Note that in the case of neutral surfaces $|f|^{=}_{\max} = 0$, which implies that forming parallel lamellae cannot reduce the surface-block interfacial energy. Perpendicular lamellae with $L = L_0$ therefore occur even at $f = 0$, induced by the hard-surface effect. Similarly, parallel antisymmetric lamellae between symmetric surfaces and parallel symmetric lamellae between antisymmetric surfaces are not preferred over perpendicular lamellae (which cost almost the same surface-block interfacial energy), even if they have a period of L_0.

In their Cahn–Hilliard calculations for antisymmetric surfaces attracting different blocks, Brown and Chakrabarti also observed perpendicular morphology when parallel antisymmetric lamellae are least favorable.[13] But their perpendicular morphology in some cases is different from well-formed perpendicular lamellae. For example, in the strong segregation regime, a weak surface potential, the lowest quench temperature, and $D/L_0 \approx 1$ ($B = 0.01$, $h = 0.1$, $\epsilon = 0.0$, and $d = 15$, respectively, in their own notation), a perpendicular lamellae-like structure was observed near each surface, but the normals of these two lamellae-like structures were orthogonal. That is, there was a ''twist'' from one orientation to the other in the middle of the confined film.[13] In contrast to these predictions, all of the perpendicular lamellae observed in our simulations were well-formed. Interestingly, we did observe comparable ''twisted'' perpendicular structures in some runs, but they only appeared as intermediate states, and evolved to well-formed perpendicular lamellae as the simulation progressed.

It is important to mention that in the case of weakly preferential surfaces, we also observed perpendicular lamellae (different from the parallel morphology illustrated in Fig. 6) in various runs for symmetric surfaces separated at $D/L_0 = 2.25$, as well as for antisymmetric surfaces separated at $D/L_0 = 2.75$ and 3. Such perpendicular lamellae may correspond to local free energy minima. Similar to the simulations in Sec. III, the energy barrier between configurations of parallel and perpendicular lamellae is so large that our system cannot overcome it in the course of a finite simulation run. Since a quantitative comparison between the free energy of these two configurations is difficult, we cannot determine without some ambiguity which morphology is more stable.

B. Density of confined thin films

As mentioned before, our simulations are performed at a specified chemical potential; it is therefore possible to study how the density of the confined thin films changes with the surface preference and the surface separation.

For the same morphology of the diblock copolymer thin films (perpendicular lamellae with $L = L_0$, or parallel lamellae with the same number of bilayers), we find that the density of the confined film $\langle \rho \rangle$ increases as the film thickness D increases. Figure 7 shows such a relationship for perpendicular lamellae. The data for symmetric and antisymmetric surfaces in Fig. 7 correspond to the case of weakly preferential surfaces. The bulk value of the density (0.8036 corresponding to $L_0 = 12$ in the bulk simulations) is represented by a dashed line; we can see that the density of the confined films is below the bulk value for all surface separations. As D increases, this confinement effect is less pronounced and the density of the films increases towards the bulk value, as shown in Fig. 7. As expected, we can also see in Fig. 7 that, for a given value of surface separation, the density of the thin film between two preferential (repulsive) surfaces is smaller than that of the film between two neutral surfaces.

Figure 8(a) shows that, for parallel lamellae with the same number of bilayers between symmetric surfaces ($n = 1$, 2, and 3), the density increases as D increases. Figure 8(a) also shows that the density slightly increases as surface-block repulsion increases. Similar results are obtained for parallel lamellae between antisymmetric surfaces, as shown in Fig. 8(b).

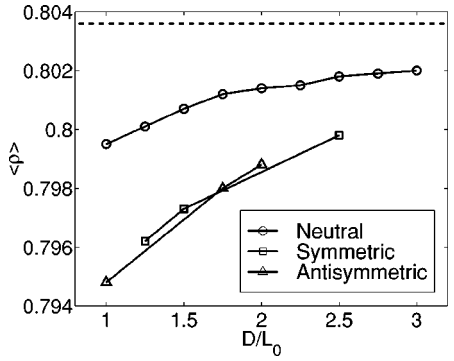

FIG. 7. Density of perpendicular lamellae confined between two neutral or (weakly) preferential surfaces. The dashed line represents the bulk density 0.8036.

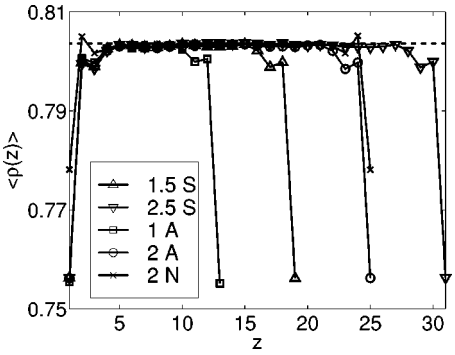

FIG. 9. Density profile of perpendicular lamellae confined between two (weakly) preferential or neutral surfaces. D/L_0 in each case is given in the legend, where ''*S*'' denotes symmetric surfaces, ''*A*'' denotes antisymmetric surfaces, and ''*N*'' denotes two neutral surfaces. The dashed line represents the bulk density 0.8036.

To understand better the behavior of the density of confined thin films, we examine the density profile along the z direction, $\langle \rho(z) \rangle$. Kikuchi and Binder[7] pointed out that, to reduce the block–block and surface–block interfacial energy, vacancies slightly accumulate at $A-B$ interfaces as well as near the surfaces. Our calculations confirm the observations of these authors. Shown in Fig. 9 are the density profiles along the z direction for perpendicular lamellae between two (weakly) preferential surfaces. The bulk value of the density (0.8036 corresponding to $L_0=12$ in the bulk simulations) is again represented by a dashed line. We can see that in the interior of the confined films the density is close to the bulk value, but near the surfaces the density decreases due to surface–block repulsion. Similar results are found for the density profiles of perpendicular lamellae between two neutral surfaces (also shown in Fig. 9 for $D/L_0=2$), where the decrease of density near the neutral surfaces is simply due to the hard-surface effect. The results for all other perpendicular lamellae observed in our simulations are comparable. From Fig. 9 we can see that in perpendicular lamellae, the density profile near the surfaces is governed by the nature of surface–block interactions.

Figure 10 shows the density profiles along the z direction, $\langle \rho(z) \rangle$, for parallel lamellae with $n=2$ between symmetric and strongly preferential surfaces. The results for all other parallel lamellae observed in our simulations are comparable. The accumulation of vacancies at the $A-B$ interfaces becomes apparent in this figure. Since such accumulation is caused by repulsion between A and B segments, the strength of the surface–block repulsion has only a slight effect on the density profiles. We find that as the surface–block repulsion increases, the density near the surfaces (at $z=1$ and L_z) follows opposite trends for perpendicular lamellae (where the density decreases) and for parallel lamellae (where the density slightly increases). This might explain why the density of parallel lamellae slightly increases as the strength of surface–block repulsion increases, as shown in Figs. 8(a) and 8(b). In addition, the frustration (stretching or compressing) of the confined parallel lamellae has obvious

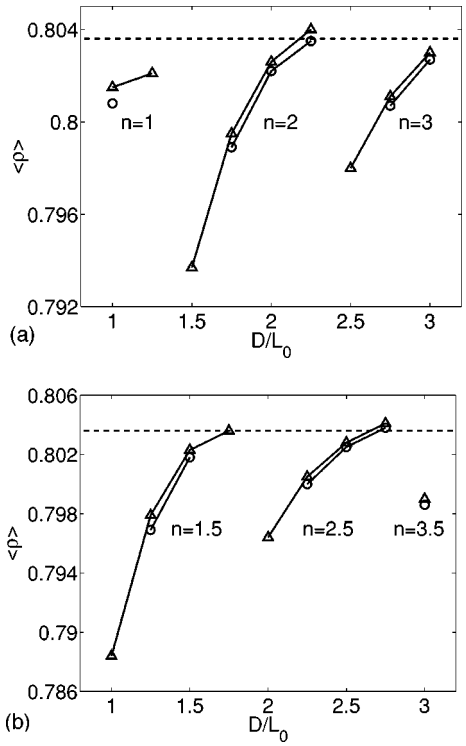

FIG. 8. Density of parallel lamellae confined between (a) symmetric surfaces; (b) antisymmetric surfaces. The symbol △ denotes the results between two strongly preferential surfaces; ○ denotes the results between two weakly preferential surfaces. The dashed line represents the bulk density 0.8036.

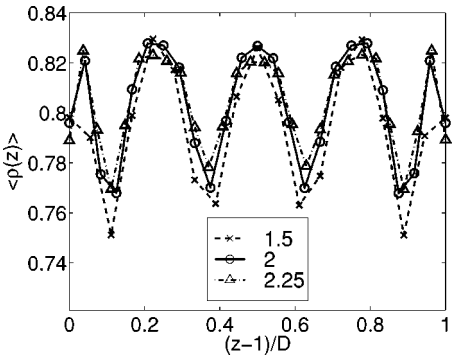

FIG. 10. Density profile of parallel lamellae with $n=2$ between symmetric and strongly preferential surfaces. The dimensionless variable $(z-1)/D$ is used to rescale the profile. D/L_0 in each case is given in the legend.

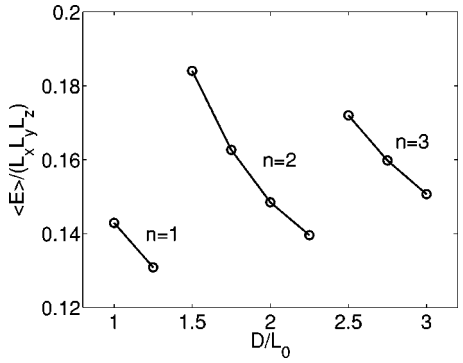

FIG. 11. Energy of parallel lamellae confined between symmetric and strongly preferential surfaces.

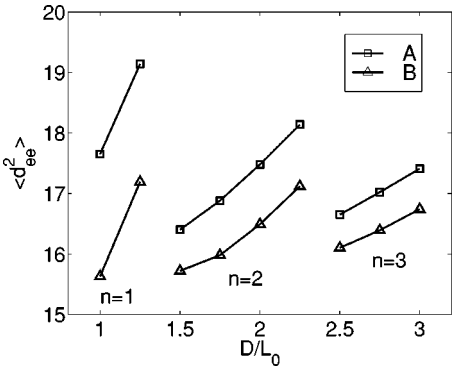

FIG. 13. Mean square end-to-end distance of blocks in parallel lamellae confined between symmetric and strongly preferential surfaces.

effects on the amplitude of density fluctuations within the film: the larger the f (not $|f|$), the smaller the amplitude. From Fig. 10, we can also see that the amplitude near the surfaces is larger than that in the interior of the film.

Figure 8(a) and 8(b) also show that the density changes discontinuously when the number of bilayers in parallel lamellae n changes. Therefore, a first-order phase transition seems to occur between the stretched and compressed parallel lamellae as the film is squeezed (and n changes). We also detected a discontinuity in the energy per unit volume, $\langle E\rangle/(L_xL_yL_z)$, when n changes. This is shown in Fig. 11 for the case of symmetric and strongly preferential surfaces.

C. Chain conformation within confined thin films

We analyze the chain conformation in the confined films by calculating the average mean square end-to-end distance of the whole chain ($\langle d_{ee}^2\rangle$), the A chain ($\langle d_{ee}^2\rangle_A$), and the B chain ($\langle d_{ee}^2\rangle_B$) in our simulations. As shown in Figs. 12 and 13, these end-to-end distances increase as D increases for given morphology of the confined films, in close analogy to the behavior of the density. For perpendicular lamellae, we can also see in Fig. 12 that, for a given surface separation, the mean square end-to-end distance of the whole chain between two (weakly) preferential surfaces is smaller than that between two neutral surfaces. It is interesting to point out the similarity between Figs. 7 and 12. For parallel lamellae with the same number of bilayers, chains go from being compressed to being stretched as D increases. Thus $\langle d_{ee}^2\rangle$, $\langle d_{ee}^2\rangle_A$, and $\langle d_{ee}^2\rangle_B$ increase. This is shown in Fig. 13 for the case of symmetric surfaces.

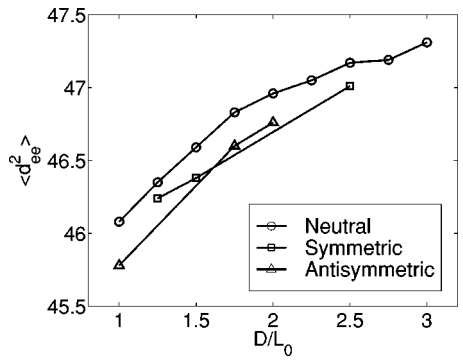

FIG. 12. Mean square end-to-end distance of chains in perpendicular lamellae confined between two neutral or (weakly) preferential surfaces.

In the case of symmetric surfaces, where A and B blocks are not interchangeable (in the sense that both surfaces consist of sB sites and therefore repel A segments), we always find that $\langle d_{ee}^2\rangle_A > \langle d_{ee}^2\rangle_B$, i.e., A blocks are stretched relative to B blocks. This is shown in Fig. 13 for the strongly preferential surfaces. Furthermore, $\langle d_{ee}^2\rangle_A - \langle d_{ee}^2\rangle_B$ is much larger in parallel lamellae than in perpendicular lamellae, where it is slightly greater than zero. In addition, for given morphology, $\langle d_{ee}^2\rangle_A$ slightly increases while $\langle d_{ee}^2\rangle_B$ slightly decreases as surface-block repulsion increases. To help explain these results, we calculate the thickness $h(i)$ of each half-layer i, numbered from 1 (closest to the lower surface) to $4n$ (closest to the upper surface), in parallel lamellae. The position of the $A-B$ interfaces in the parallel lamellae is determined by $\langle \rho_A(z)-\rho_B(z)\rangle = 0$, and the thickness of the two half-layers constituting the A-rich or B-rich domains (except those closest to the surfaces) are set to be equal. (Here we assume that the thickness of $A-B$ interfaces is zero.) Shown in Fig. 14(a) are the results for the unfrustrated parallel lamellae (i.e., $f=0$) confined between two strongly preferential surfaces. We can see that the thickness of the half-layers within the confined parallel lamellae is different. The two half-layers closest to the surfaces are thinner than those in the interior of the confined film. Furthermore, we found that $h(1)$ [and $h(4n)$] slightly decreases as surface-block repulsion increases. For symmetric $sB-sB$ surfaces the two half-layers closest to the surfaces consist mainly of B blocks; the behavior of the mean square end-to-end distance of A and B blocks can now be understood, by relating these end-to-end distances to the thickness of the half-layers.

Shown in Fig. 14(b) is the thickness of the half-layers within parallel lamellae of $n=1.5$ (between antisymmetric surfaces) and $n=2$ (between symmetric surfaces) confined between two strongly preferential surfaces. We can see that $h(1)$ [and $h(4n)$] increases as f increases, and that the half-layers in the interior of the confined parallel lamellae may also have slightly different thicknesses. We obtain similar results for all other parallel lamellae studied in this work.

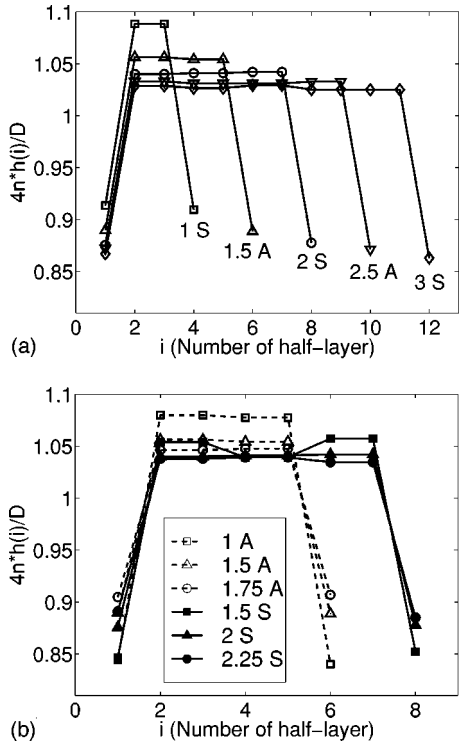

FIG. 14. Thickness of half-layers within parallel lamellae confined between two strongly preferential surfaces: (a) $f=0$; (b) $n=1.5$ (between antisymmetric surfaces) and $n=2$ (between symmetric surfaces). i is the number of half-layer in parallel lamellae, ordered from 1 (closest to the lower surface) to $4n$ (closest to the upper surface). D/L_0 in each case is given in the figure, where ''*S*'' denotes symmetric surfaces, and ''*A*'' denotes antisymmetric surfaces.

D. Surface-induced preferential segregation of segments in perpendicular lamellae

The formation of perpendicular lamellae between two (weakly) preferential surfaces is accompanied by a segregation of preferred segments near the corresponding surfaces. Such a segregation lowers the surface–block interfacial energy induced by perpendicular lamellae. Shown in Fig. 15 are the order parameter profiles in the z direction ($\langle \rho_A(z) - \rho_B(z) \rangle$) for perpendicular lamellae between symmetric surfaces separated by $D/L_0=1.5$ and antisymmetric surfaces separated by $D/L_0=2$. From Fig. 15 we can see the segregation clearly. We observe similar results for all other cases studied here. This surface-induced preferential segregation of segments in perpendicular lamellae was also observed by Brown and Chakrabarti.[13] The peaks of $\langle \rho_A(z) - \rho_B(z) \rangle$ shown in Fig. 15 (at $z=5$ and 15 in the case of symmetric surfaces and at $z=5$ and 21 in the case of antisymmetric surfaces) indicate that such a segregation causes some oscillation of the $A-B$ interfaces in perpendicular lamellae. This is consistent with self-consistent-field calculations.[8,9] This issue is addressed in more detail in Ref. 19.

V. COMPARISON WITH EXPERIMENTAL RESULTS

Having discussed the general trends observed in our simulations, we now proceed to qualitatively compare our simulation results with those found experimentally.[1–5] A quantitative comparison is difficult because translating our surface–block interactions into specific experimental systems introduces some degree of ambiguity. Also, our chain length is relatively short compared to the copolymers used in the experiments.

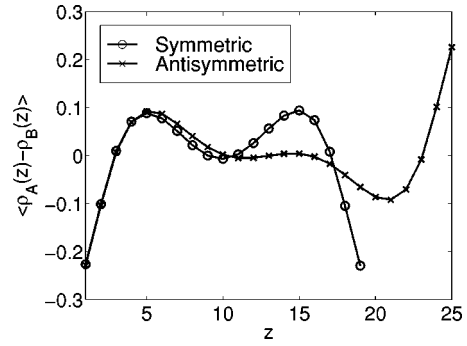

FIG. 15. Surface-induced segregation of preferred segments in perpendicular lamellae confined between two (weakly) preferential surfaces. $D=18$ $(1.5L_0)$ for symmetric surfaces, and $D=24$ $(2L_0)$ for antisymmetric surfaces.

A. Parallel lamellae between two strongly preferential surfaces

We have seen in Sec. IV that in the case of symmetric and strongly preferential surfaces, we always observed parallel lamellae with an integer number of bilayers. The period of the confined parallel lamellae L can deviate from the bulk value L_0 to accommodate the frustration between the surface separation D and L_0. The confined lamellae are compressed and stretched in a cyclic manner as a function of D. These are in agreement with experimental evidence.[1–3]

B. Perpendicular lamellae between two neutral surfaces

In their experiments, Kellogg *et al.* confined symmetric diblock copolymers between two hard surfaces coated by a layer of random copolymers to reduce the surface preference.[3] Their results for the sample with $D/L_0=2.52$, where the maximum frustration between D and L_0 occurs, suggested a perpendicular ordering of lamellae near at least one surface.[3] However, the results for the sample with $D/L_0=2.80$ showed no sign of perpendicular lamellae.[3] As discussed in Sec. IV A, perpendicular lamellae are preferred by two neutral and hard surfaces, regardless of surface separation. This is also predicted by self-consistent-field calculations.[8,9] Pickett and Balazs argued that the surface preference may not be completely absent in the experiment, which could explain the discrepancy between the calculations and the experiment.[8] If this was the case, the experimental results would be in agreement with our simulations for symmetric and weakly preferential surfaces. Another possible reason could be that the random copolymers were not grafted in the experiment, and they could diffuse into the layer of diblock copolymers in the middle to cause unexpected results.[5]

To clarify this ambiguity, Huang *et al.*[5] grafted random copolymers P(S-r-MMA) onto silicon wafers to construct lower neutral surfaces. Perfluorodecanoyl moieties were

chemically end-linked to P(S-r-MMA) having the same composition as those grafted onto silicon wafers. The strong segregation of the perfluorodecanoyl terminated random copolymers to the polymer/air interface (due to the low surface energy of fluorinated groups) produced another neutral surface on the top. Through this strategy, diblock copolymers can be effectively trapped between two random copolymer brushes considered to be neutral.[5] Thin films of symmetric diblock copolymer dPS-PMMA confined between three different surface configurations were prepared: two neutral surfaces, a lower neutral surface and an upper free surface (air), and a lower silicon substrate and an upper neutral surface. The thickness of the confined diblock copolymer films was $4.72L_0$ for all these samples.[5] Perpendicular lamellae were found throughout the entire film in the case of two neutral surfaces. Similar to the results in Ref. 3 and 4, the orientation of the perpendicular lamellae was found to be short-ranged.[5] For the film between a lower neutral surface and an upper free surface, since PS blocks are preferred by air, no perpendicular lamellae were observed appreciably from the top until 600 Å of the film was removed ($L_0 \approx 360$ Å in their experiments).[5] For the film between a silicon substrate and a neutral surface on the top, parallel lamellae predominated throughout the entire film due to the strong preference of PMMA blocks by the silicon substrate.[5]

Consistent with the above experimental results, we observed perpendicular lamellae throughout the entire film in our simulation for symmetric diblock copolymers confined between two neutral surfaces separated at $D/L_0=4.75$. As we changed the lower neutral surface to a strongly preferential sB surface ($\epsilon_{sB-A}=2\epsilon_{A-B}$) representing the silicon substrate in the experiment, we observed some mixed morphology of about two bilayers of parallel lamellae near the sB surface and perpendicular lamellae near the neutral surface, as shown in Fig. 16. Similar morphology was observed even as we increased the preference of the sB surface to be $\epsilon_{sB-A}=9\epsilon_{A-B}$. This morphology is more similar to that observed between the neutral surface and air in the experiment (except that the preferential surface was a free surface in that case). As we pointed out before, the formation of perpendicular lamellae near neutral surfaces is induced by the hard-surface effect; the upper neutral surface produced in the experiment may not be providing a geometrical confinement such as that of a hard surface. It was therefore unable to prevent the formation of parallel lamellae throughout the entire film.

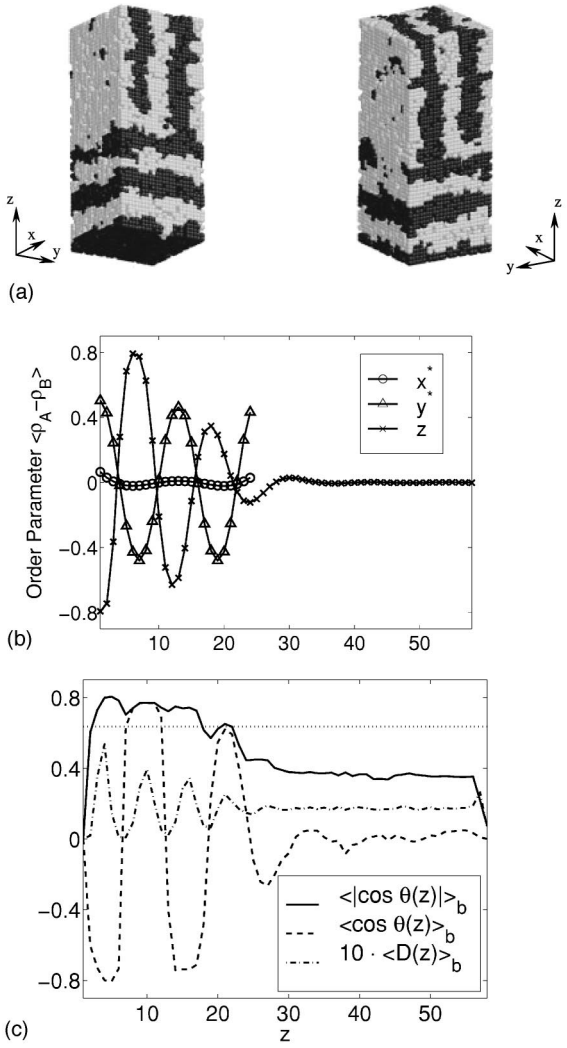

FIG. 16. Mixed morphology between sB-neutral surfaces at $D/L_0=4.75$. About two bilayers of parallel lamellae form near the lower strongly preferential sB surface, and perpendicular lamellae form near the upper neutral surface. (a) Snapshot of the system configuration. Light regions represent A blocks and dark regions represent B blocks. (b) Order parameter profiles. (c) Chain orientation and center-of-mass distribution profiles. The dotted line represents the criterion between the perpendicular and parallel orientations of chains: $\langle|\cos\theta(z)|\rangle_b=(1/\pi)\int_0^\pi|\cos\theta|d\theta=2/\pi$.

C. Mixed morphology between strongly asymmetric surfaces

A mixed morphology was also found in the experiments of Koneripalli *et al.*, where symmetric diblock copolymers of poly(styrene-d_8)-poly(2-vinylpyridine) (dPS-PVP) were confined between two dissimilar surfaces: an oxide-stripped silicon wafer (Si) and a glassy polymer poly(2-methylvinylcyclohexane) (P2MVCH).[4] PS blocks are preferred by Si, while PVP blocks are preferred by P2MVCH. The mixed morphology of basically perpendicular lamellae near the P2MVCH surface and parallel lamellae near the Si surface was reported for the samples of $D/L_0=0.98\sim1.25$.[4] The authors argued that the difference between the dPS/P2MVCH and PVP/P2MVCH interfacial tensions is smaller than that between the dPS/Si and PVP/Si interfacial tensions, and this leads to the mixed morphology in the case of strong frustration between D and L_0. For the samples of $D/L_0=1.31\sim1.47$, only parallel lamellae were observed.[4]

The experiments of Koneripalli *et al.* suggest that such mixed morphology is a result of asymmetric (not antisymmetric) surface–block interactions.[4] We therefore performed Monte Carlo simulations of symmetric diblock copolymers confined between two dissimilar hard surfaces: a lower sB surface and an upper sA surface. We set the asymmetric surface–block interactions to be $\epsilon_{sA-B}=0.4\epsilon_{A-B}$ and $\epsilon_{sB-A}=\epsilon_{A-B}$. If we represent the PS blocks as A, the PVP blocks as B, the P2MVCH surface as sA, and the Si surface as sB, we can see that our parameters qualitatively correspond to

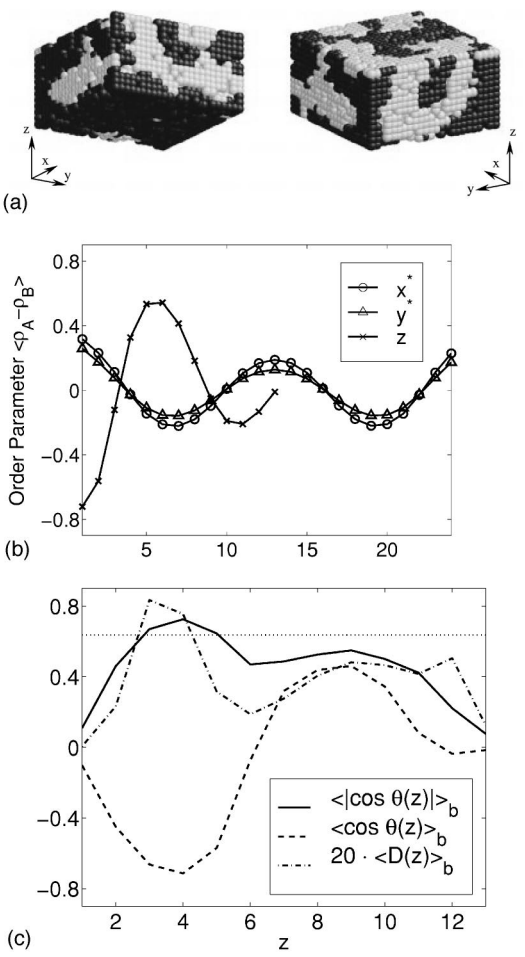

FIG. 17. Mixed morphology between asymmetric surfaces at $D/L_0=1$. About one layer of parallel lamellae form near the lower *sB* surface, and both *A* and *B* segments in nearly the same amount exist near the upper *sA* surface. Chains tend to orient parallel to the surfaces in the upper part of the film. Refer to Fig. 16 for more explanations.

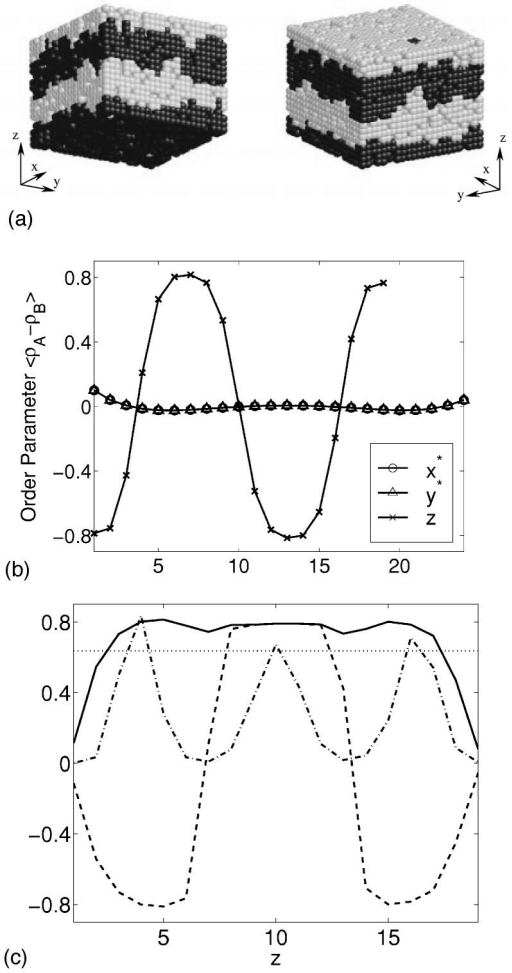

FIG. 18. Parallel lamellae with $n=1.5$ between asymmetric surfaces at $D/L_0=1.5$. Refer to Fig. 16 for more explanations. The legend in (c) is the same as in Fig. 17(c).

the system studied in Ref. 4, i.e., $|\epsilon_{\text{dPS-P2MVCH}}-\epsilon_{\text{PVP-P2MVCH}}|<|\epsilon_{\text{dPS-Si}}-\epsilon_{\text{PVP-Si}}|$.

The resulting structures for $D/L_0=1$ and 1.5 are shown in Figs. 17 and 18, respectively. From Fig. 17 we can see that parallel lamellae (about one layer of chains perpendicular to the surfaces) form near the lower *sB* surface, and that both *A* and *B* segments in nearly the same amount exist near the upper *sA* surface, as indicated by the order parameter profile along the *z* direction. Although the chains tend to orient parallel to the surfaces in the upper part of the film, as indicated by $\langle|\cos\theta(z)|\rangle_b$, the morphology in that region does not correspond to well-developed perpendicular lamellae. This may be caused by the complex morphology at the ''combined'' region in the middle of the film, as well as the relatively small film thickness. (Our simulations indicate that it is difficult to simulate confined films of thickness smaller than L_0.) However, as shown in Fig. 16, we did observe some mixed morphology between two strongly asymmetric (*sB*-neutral) hard surfaces separated at $D/L_0=4.75$. On the other hand, for $D/L_0=1.5$, we observed 1.5 bilayers of parallel lamellae throughout the entire film. This is consistent with the experimental results.

Matsen predicted that a mixed morphology is not the most thermodynamically stable state for symmetric diblock copolymers confined between two hard and homogeneous surfaces, regardless of the surface-block interactions.[9] We agree with this in the case of symmetric and antisymmetric surfaces, where the strength of the surface preference is identical for the two surfaces. As can be seen in Sec. IV, mixed morphology was not observed as a stable state in such simulations. We also pointed out in Sec. III that the mixed morphology observed by Kikuchi and Binder in their simulations of two identical (symmetric) surfaces[7] might be a result of the mismatch between the bulk lamellar period and the simulation box size employed in their work. However, when the two surfaces are strongly asymmetric (such as the case of *sB*-neutral surfaces simulated above), a mixed morphology could be thermodynamically stable. Unfortunately, in the case of symmetric diblock copolymers confined between asymmetric (not antisymmetric) surfaces, the mixed morphology was not examined *numerically* by Matsen in his paper.[9] Such a calculation would be very helpful.

VI. SUMMARY

Thin films of symmetric diblock copolymers confined between two hard, homogeneous and parallel surfaces were

investigated with Monte Carlo simulations on a simple cubic lattice. For simulations of lamellar structures using periodic boundary conditions, the match between bulk lamellar period L_0 and the simulation box size is crucial to obtain meaningful results. The simulations were performed in an expanded grand-canonical ensemble, where the chemical potential and the temperature of the confined films are specified and the density is allowed to fluctuate. The morphology, density, and chain conformations within the films were studied systematically as a function of the film thickness and the strength of surface preference.

The observed morphology is the result of a delicate balance among block–block interfacial energy, surface–block interfacial energy, and elastic energy (conformational entropy) of the system. The equilibrium morphology of the diblock copolymers is a strong function of the interfacial properties and the separation distance D of the confining surfaces. Near homogeneous surfaces with strong preference to one of the two blocks, lamellae tend to orient parallel to the surfaces to reduce the surface–block interfacial energy. Near neutral surfaces, which have no preference to either one of the two components, the confinement of hard surfaces induces the formation of perpendicular lamellae of the bulk period. Therefore, parallel and perpendicular lamellae, depending on the strength of surface preference and the frustration between D and L_0, were observed between the symmetric (two identical surfaces repelling one of the two blocks) and the antisymmetric (two surfaces repelling different blocks with the same strength of surface-block interactions) homogeneous surfaces, as summarized in Fig. 6. The number of bilayers of parallel lamellae n is always an integer (parallel symmetric lamellae) in the case of symmetric surfaces or half an odd integer (parallel antisymmetric lamellae) in the case of antisymmetric surfaces. In parallel lamellae, any frustration between D and L_0 is accommodated by deviations of L from L_0. The elastic energy (conformational entropy) cost for such deviations is minimized by choosing an appropriate value of n. However, there exists a maximum extent to which the lamellae can be compressed or stretched by the surfaces. Over this limit, the diblock copolymers change their orientation to form perpendicular lamellae of $L=L_0$, at the lesser cost of increasing the surface–block interfacial energy. For two asymmetric (not antisymmetric) homogeneous surfaces we observed, under certain conditions, mixed morphology consisting of parallel lamellae near one surface and perpendicular lamellae near the other surface. The results of our simulations are qualitatively consistent with experimental results.

For the same morphology of the diblock copolymer thin films (perpendicular lamellae with the bulk period, or parallel lamellae with the same number of bilayers n), we found that, at constant chemical potential and temperature, the density of the confined film increases as D increases. As the surface–block repulsion increases, the density near the surfaces follows opposite trends for perpendicular lamellae (where the density decreases) and for parallel lamellae (where the density slightly increases). Within the confined film, a slight accumulation of vacancies (unoccupied lattice sites) was observed at $A-B$ interfaces, as well as near the surfaces, which reduces the block–block and surface–block interfacial energy of the system, respectively. This accumulation gives rise to density fluctuations along the z direction within the parallel lamellae. The frustration (stretching or compressing) of the confined parallel lamellae has obvious effects on the amplitude of such fluctuations: the larger the f (not $|f|$), the smaller the amplitude. We also found that the amplitude near the surfaces is larger than that in the interior of the film. From the discontinuity of the density and the energy per unit volume of the system, it could be argued that a first-order phase transition occurs between stretched and compressed parallel lamellae with different n.

The mean square end-to-end distances (for the whole chain, the A chain, and the B chain) increase as D increases for given morphology of the confined films, in close analogy to the behavior of the density. For a given film thickness and perpendicular lamellae, we also found that the mean square end-to-end distance between two (weakly) preferential surfaces is smaller than that between two neutral surfaces. For parallel lamellae, we found that the two half-layers closest to the surfaces are $10\sim15\,\%$ thinner than those in the interior of the confined film. The thickness of these two half-layers increases as f increases.

The formation of perpendicular lamellae between two (weakly) preferential surfaces was accompanied by a segregation of preferred segments near the corresponding surfaces. Such a segregation lowers the surface–block interfacial energy induced by perpendicular lamellae, and causes some oscillation of the $A-B$ interfaces in the perpendicular lamellae.

Note added in proof. After submission of this paper, a Monte Carlo study of confined copolymers between neutral surfaces was reported by Sommer *et al.* [J. U. Sommer *et al.*, J. Chem. Phys. **111**, 3728 (1999)]. Their simulations were performed in a canonical ensemble in the framework of the bond fluctuation model. For those cases where a comparison could be made between their work and ours, these authors reported findings that are consistent with ours.

ACKNOWLEDGMENTS

Financial support for this work was provided by the Semiconductor Research Corporation through contract No. 99-LP-452 and by the NSF CTS-9703207 and CTS-9901430. J.J.dP. is grateful to Gustavo Chapela for his hospitality during a sabbatical visit to the Mexican Petroleum Institute.

[1] P. Lambooy *et al.*, Phys. Rev. Lett. **72**, 2899 (1994).
[2] N. Koneripalli *et al.*, Macromolecules **28**, 2897 (1995).
[3] G. J. Kellogg *et al.*, Phys. Rev. Lett. **76**, 2503 (1996).
[4] N. Koneripalli *et al.*, Langmuir **12**, 6681 (1996).
[5] E. Huang *et al.*, Macromolecules **31**, 7641 (1998).
[6] M. Kikuchi and K. Binder, Europhys. Lett. **21**, 427 (1993).
[7] M. Kikuchi and K. Binder, J. Chem. Phys. **101**, 3367 (1994).
[8] G. T. Pickett and A. C. Balazs, Macromolecules **30**, 3097 (1997).
[9] M. W. Matsen, J. Chem. Phys. **106**, 7781 (1997).
[10] K. R. Shull, Macromolecules **25**, 2122 (1992).
[11] M. S. Turner, Phys. Rev. Lett. **69**, 1788 (1992).

[12] D. G. Walton *et al.*, Macromolecules **27**, 6225 (1994).
[13] G. Brown and A. Chakrabarti, J. Chem. Phys. **102**, 1440 (1995).
[14] F. A. Escobedo and J. J. de Pablo, J. Chem. Phys. **105**, 4391 (1996).
[15] Q. Yan and J. J. de Pablo (unpublished).
[16] K. Binder and H. Fried, Macromolecules **26**, 6878 (1993).
[17] R. G. Larson, Macromolecules **27**, 4198 (1994).
[18] U. Micka and K. Binder, Macromol. Theory Simul. **4**, 419 (1994).
[19] Q. Wang *et al.*, J. Chem. Phys. (submitted).